IEEE Access
Multidisciplinary | Rapid Review | Open Access Journal

Received May 16, 2020, accepted May 22, 2020, date of publication May 26, 2020, date of current version June 30, 2020.

Digital Object Identifier 10.1109/ACCESS.2020.2997676

Modeling Simulation and Temperature Control on Thermal Characteristics of Airborne Liquid Cooling System

ZHANGZHI DONG, XIAOGANG LI, ZHE LI, AND YANYAN HOU
Aeronautics Engineering College, Air Force Engineering University, Xi'an 710038, China
Corresponding author: Zhe Li (lizhe08402@163.com)

This work was supported by the National Natural Science Foundation of China under Grant 61873351.

ABSTRACT Aiming at the temperature control of the liquid cooling system of aircraft electronic equipment, the thermal characteristics of the system under different temperature conditions are analyzed through model simulation, and a calculation method is given for the thermal design of the liquid cooling system. This paper simplifies the system and establishes a numerical calculation model for the heat transfer of the main components (such as liquid storage tanks, gear pumps, radiators, etc.). The temperature changes in the main components of the system within the operating temperature range of the system (−40 °C-50 °C) were calculated, and the thermal characteristics of the cold plate were obtained by using the AMESim software. Further, temperature control schemes of several liquid cooling systems are compared for their working efficiency under low temperature and over-temperature conditions based on the original model. The results show that the temperature index of the airborne liquid cooling system basically meets the technical requirements of the cold plate inlet temperature (5 °C-30 °C) under typical operating conditions. Under low-temperature conditions, the rapid heating of the cold plate can be achieved through the electric heater control scheme. Under high-temperature circumstances, opening the ram air port scheme has a better cooling effect than increasing the fan speed scheme, but the former needs to consider the flight conditions to avoid the cold plate temperature exceeding the target range.

INDEX TERMS Liquid cooling system, aerospace simulation, electronics cooling, thermal analysis, temperature control.

I. INTRODUCTION

With the increasing demand for equipment in the aviation field, traditional airborne cooling equipment is constantly updated and improved. In the case of large heat flux dissipation, traditional convective heat dissipation or forced air cooling are used in the past, resulting in low heat dissipation efficiency and insufficient temperature control precision [1], [2]. The heat transfer coefficient and specific heat capacity of the liquid are much larger than that of air, and have a higher cooling efficiency [3]. According to the literature [4], the water-cooled heat transfer coefficient is much larger than the air-cooled heat transfer coefficient——the approximate range of gas forced convection heat transfer coefficient is 20∼100 W/(m^2·K), and the heat transfer coefficient of forced convection of water is up to 15000 W/(m^2·K).

The associate editor coordinating the review of this manuscript and approving it for publication was Christopher Kitts.

The air-cooled heat dissipation system is mainly composed of a fan and a radiator [5]. It depends on the forced air cooling of the fan and the internal structure of the radiator. Its essence is the direct heat exchange between the air and the device. Aircraft air cooling system or liquid cooling system can be used to cool electronic equipment. For electronic equipment with low heat flux density, an air cooling system can be used, and a fan or cooling air can be specially extracted from the aircraft's environmental control system to cool the electronic equipment. For electronic equipment with high heat flux density, if the air cooling method is adopted, many problems are difficult to solve. The first is that the use of air as a cooling medium cannot meet the requirements of high heat flux heat transfer of electronic equipment; second, some engines cannot provide an excessively high air intake for the air cooling system [6]. Besides, due to the small space in the equipment compartment, it is difficult to arrange the air cooling pipes in the electronic equipment cabinet.

Thus, using an airborne liquid cooling system to cool the avionic electronic equipment (e.g., radar), and using liquid cooling instead of air cooling can achieve efficient and reliable heat regulation [11] below [7]–[11].

For the study of the liquid cooling system and its cooling efficiency, TomLee *et al.* came up with the concept of the compact liquid cooling system earlier and proposed the design criteria and improved methods for the compact liquid cooling system, which could improve the thermal performance of the system by selecting high-pressure fans and improving heat exchange efficiency and the 5.5-liter system can remove up to 274 W of power from the inlet liquid to the air, reducing the temperature by 52 degrees Celsius [12]. Nguyen *et al.* studied a nanoparticle-water mixture used in cooling microprocessors or other electronic components [13]. Experiments showed that the heat transfer coefficient increased by 40% compared to the base fluid, the particle concentration increased, and the temperature of the heated component decreased [14]. Zhu *et al.* designed a liquid cooling control system using a single emergency and integrated digital IC acquisition control system, which reduced the cost of this type of liquid cooling system by 60% [15]. Kim *et al.* analyzed the influence of a hybrid cooling system on the cooling performance of large power transformers and its cooling performance is about 22% higher than the worst cooling performance at all flow rates [16].

In the simulation research of the liquid cooling system, with the help of EASY5 software, Jin *et al.* built the dynamic mathematical model of the fighter evaporative refrigeration system and analyzed the dynamic performance of the system [17]. Li *et al.* established a mathematical model for the gas-liquid plate-fin heat exchanger with large thermal inertia and calculated and analyzed the temperature characteristics of single-flow and three-flow heat exchangers with Matlab [18]. Li *et al.* used Matlab/Simulink to analyze the influence of different parameter steps on the performance of airborne evaporative cycle refrigeration systems [19]. Zuo *et al.* built an airborne liquid cooling system model based on AMESim, and mainly introduced the establishment process of the software platform, and made a simple calculation and analysis [20]. Marcinichen *et al.* built the simulation model of gas-liquid two-phase liquid cooling system by using the two-phase flow simulation code compiled by themselves [21]. In terms of liquid cooling simulation, they all provide references that can be used for reference, especially Marcinichen *et al.* have established a two-phase flow simulation model, which can well simulate the actual working situation of the system.

In the field of aviation applications, Birur *et al.* studied a liquid cooling system based on a micro-mechanical pump to realize the thermal control of micro spacecraft with a power heat flow rate exceeding 25W/cm^2 [22]. Zhu *et al.* developed a new type of liquid cooling system consisting of a cooling subsystem, circulation system, and monitoring subsystem for high power and high heat flow avionics equipment [6]. Pal *et al.* summarized various thermal management

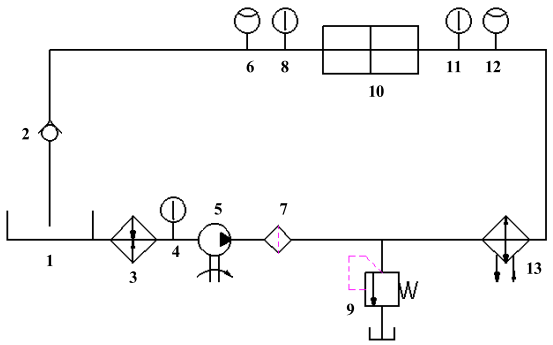

1—liquid storage tank; 2—backflow check valve; 3—electric heater; 4,8,11— temperature sensor; 5—gear pump ; 6,12—flow sensor; 7—filter; 9—relief valve; 10—cold plate; 13—plate-fin heat exchanger

FIGURE 1. Liquid cooling system schematic.

architectures of aircraft electronic cooling, introduced the advantages and disadvantages of several typical cooling schemes, and gave simulation examples of thermal analysis and flow analysis of motor controllers [23]. The research of liquid cooling systems in the civil field develops from the pursuit of refrigeration efficiency to the consideration of miniaturization and high reliability of liquid cooling equipment. However, there are relatively few studies on the application of the liquid cooling systems in the field of aviation. With the multi-function and complexity of airborne electronic equipment, the cooling demand for the system is increasing day by day. It is necessary to replace the traditional forced air-cooling with efficient and reliable liquid cooling. Therefore, from the perspective of heat transfer, the research of modeling and simulation on thermal characteristics of the high heat flux components of the system is of great help to the design and practical use of the liquid cooling system.

This article establishes a mathematical model of the main components of the system with a large thermal load, and uses the AMESim multidisciplinary software to perform the calculation of the thermal characteristics of the entire system. The dynamic thermal characteristics of the liquid cooling system under several typical system temperature conditions are obtained through simulation. The temperature feedback control of the liquid storage tank and heat exchanger is realized through the software state machine module. The research provides a more comprehensive system thermal simulation model and calculation method, which can provide a reference for the engineering design, test verification, and system optimization of the airborne liquid cooling system.

II. MATHEMATICAL MODEL OF SYSTEM THERMAL CHARACTERISTICS

To simplify the system, we consider the main factors and functional components that have a large impact on the thermal characteristics of the liquid cooling system. The system schematic is shown in Figure 1.

In the liquid cooling circuit, the liquid storage tank is used to store the coolant required for the system to work cyclically. The booster pump uses a small flow gear pump

driven by a motor, and the component model in AMESim can be used to simulate the pressure and flow characteristics of the pump. During the working process of the gear pump, the dry friction and constant friction of the pump will cause mechanical losses. When the various components in the pump are relatively moved, they are lubricated and cooled by the coolant. It can be considered that the heat generated by the mechanical loss acts on the coolant, and the coolant is forced to convection heat exchange with the shell. At the same time, the shell performs radiative heat exchange and natural convection heat exchange with the environment. The relief valve plays a protective role and relieves the excessive pressure of the system. The heat exchanger uses a plate-fin radiator, and its own heat exchanger in AMESim is used to simulate its working conditions. The hot-side fluid is liquid and the cold-side fluid is air. An axial fan is used to force cool the radiator. The axial fan is installed at the air outlet of the cold side of the radiator and is used for forced air cooling of the radiator. The anti-overflow device is installed on the pressurized air line of the liquid storage tank to prevent the liquid in the liquid storage tank from flowing back into the pressurized air line during the aircraft maneuvering flight. The check valve is used to simulate the anti-overflow device in AMESim.

The entire liquid cooling system uses No.65 cooling liquid (60% ethylene glycol) as the heat conduction medium [24]. The clb-7 liquid cooling pump is used to output the cooling liquid in the storage tank. The cooling liquid is forced air-cooled by a plate-fin heat exchanger. After heat dissipation, it is sent to the cold plate to cool the airborne electronic equipment, and then returns to the liquid storage tank. An axial fan is installed at the cold side air outlet of the heat exchanger to force the heat exchanger to air-cool.

The maximum flow of the cold plate during the system's operation is 12 L/min, and the heat generation power of the airborne equipment (cold plate heat generation power) is 2000 W. The main components of the heat load included in the liquid cooling system are the liquid storage tank, the gear pump, and the heat exchanger, electric heater, cold plate, and pipeline. The thermal characteristic model of components are divided into the following five sections. The heat transfer formulas in this article mainly refer to [4] and [25].

To simplify the simulation of physical problems, the following assumptions are made: 1) The flow of coolant is one-dimensional along the axial direction. 2) The volatilization of the coolant is not considered. 3) The fluid in the pipeline is incompressible. 4) Ignoring the impact of aircraft maneuvering on the flow of coolant. 5) There is no heat loss between the heat exchanger fin and the environment. 6) we use the liquid properties of the initial temperature of the coolant, such as viscosity, density, specific heat, and thermal conductivity, without considering the properties of the fluid when the temperature changes.

A. THERMAL CHARACTERISTICS MODEL OF GEAR PUMP

Gear pump is used to provide cooling flow to the system. The fixed power is 150 W, and all the heat is lost during the working process. The pump casing performs radiative and convective heat exchange with the air. The heat transfer principle of the gear pump is shown in Figure 2.

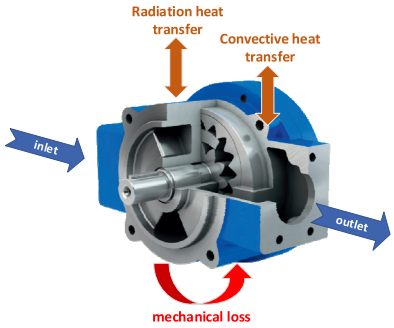

FIGURE 2. Heat transfer principle of gear pump.

The Nusselt number of the pump casing and the coolant convective heat exchange is [4]:

$$Nu = 0.023Re^{0.8}Pr^{0.33} \tag{1}$$

The Nusselt number of the shell's natural convective heat exchange with the outside world is [4]:

$$Nu = 2 + \frac{0.589Ra^{1/4}}{\left[1 + (0.469/Pr)^{9/16}\right]^{4/9}} \tag{2}$$

where, *Pr*, *Re and Ra* respectively represent Prandtl number, Reynolds number, Rayleigh number.

The expression of radiant heat transfer between the shell and the external environment is:

$$\dot{Q} = \varepsilon\sigma A\left(T^4 - T_{env}^4\right) \tag{3}$$

where, σ represents Stefan-Boltzmann constant, ε represents surface emissivity, T indicates case temperature, T_{env} indicates external temperature.

B. THERMAL CHARACTERISTICS MODEL OF PLATE-FIN HEAT EXCHANGER

The Reynolds number of the coolant flow can be expressed as:

$$Re = \frac{Q_o d_o}{A_o \nu_o} \tag{4}$$

Reynolds number characterizing fluid flow. Where, d_0 is the equivalent diameter of the internal pipe of the heat exchanger, Q_0 is coolant flow, A_0 is the cross-sectional area of the pipeline, v_0 is kinematic viscosity for coolant.

The expression of Nusselt number and Stanton number for convective heat transfer between liquid and tube wall is [25]:

$$\begin{cases} Nu = 0.245Re^{0.6}Pr^{1/3} \\ St = 0.245Re^{-0.4}Pr^{-2/3} \end{cases} \tag{5}$$

Prandtl number indicates the relationship between the temperature boundary layer and the flow boundary layer, and

reflects the influence of fluid physical properties on the convective heat transfer. Nusselt number, a quasi-number, indicating the intensity of convective heat transfer. The Rayleigh number is the product of the Grashof number and the Prandtl number, where the Grashof number describes the relationship between the buoyancy and viscosity of the fluid.

The Reynolds number of air flow can be expressed as:

$$Re = \frac{Q_a d_a}{A_a v_a} \tag{6}$$

where, Q_a is cold-side (air) flow, d_a is the cold-side equivalent diameter, v_a is the kinematic viscosity of the cold side, A_a is the circulation area of the cold side.

The Nusselt number of cold side air and hot side fin convection heat transfer can be expressed as [25]:

$$Nu = 6\left(\frac{Re}{1000}\right)^{2/3} \tag{7}$$

Total heat transfer coefficient can be expressed as:

$$\frac{1}{kA} = \frac{1}{A_o\alpha_1} + \frac{1}{A_a\alpha_2} \tag{8}$$

where, A_0 is the heat exchange area of the hot side (coolant), α_1 is the hot-side heat transfer coefficient, A_α is the cold-side heat exchange area, α_2 is the cold-side heat transfer coefficient.

Expression of the number of heat transfer units can be expressed as:

$$NTU = \frac{kA}{\min\left(\dot{m}_o C_{po}, \dot{m}_a C_{pa}\right)} \tag{9}$$

where, $\dot{m}_0$ is hot-side mass flow, $\dot{m}_\alpha$ is the cold side mass flow, C_{p0} is the specific heat of the hot side, $C_{p\alpha}$ is the specific heat of the cold side.

The expression of heat exchanger efficiency is:

$$\eta = 1 - \exp\left[\left(\frac{1}{Cr}\right) NTU^{0.22}\left\{\exp\left[-CrNTU^{0.78}\right] - 1\right\}\right] \tag{10}$$

where, $Cr = \frac{\min(\dot{m}_o C_{po}, \dot{m}_a C_{pa})}{\max(\dot{m}_o C_{po}, \dot{m}_a C_{pa})}$.

The expression of heat exchange capacity of the heat exchanger is:

$$\phi = \eta \min(\dot{m}_o C_{po}, \dot{m}_a C_{pa})\left(T'_o - T'_a\right) \tag{11}$$

where, T'_o is the hot side inlet temperature, T'_a is the cold side inlet temperature.

C. THERMAL CHARACTERISTICS MODEL OF COLD PLATE

When the coolant flows through the cold plate, it will cool the cold plate. The heat exchange power is 2000 W, here the cold plate is simplified as a simple heat exchange element, that is, heat exchanged by the cold plate is used for the temperature rise of the cooling liquid. The mathematical model of the cold plate can be expressed as:

$$T_o = T_i + \frac{W}{q_1 \rho_1 C_p} \tag{12}$$

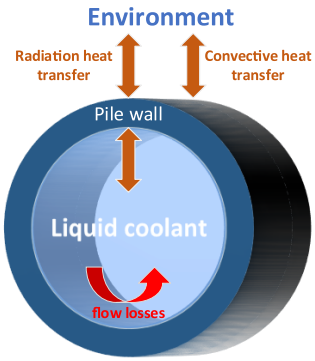

FIGURE 3. Heat transfer principle of pipelines.

where, T_i is the coolant inlet temperature, T_o is the coolant outlet meant temperature, W is heat exchange power, q_1 is coolant flow, ρ_1 is the coolant density, C_p is the specific heat of the coolant.

D. THERMAL CHARACTERISTICS MODEL OF LIQUID STORAGE TANK

The liquid storage tank is used to store the cooling liquid. Its thermal characteristics are mainly reflected in the convective heat exchange between the cooling liquid and the liquid storage tank, and the convective environment and radiant heat transfer between the liquid storage tank and the external environment.

The Nusselt number expression for forced convective heat transfer between the storage tank and the internal coolant is:

$$Nu = 0.027Re^{0.8}Pr^{0.33} \tag{13}$$

The Nusselt number expression for the natural convection heat transfer between the storage tank and the outside air is:

$$Nu = 0.48\,(PrGr)^{0.25} \tag{14}$$

where, Gr is Grashof number.

The expression of the radiant heat transfer between the storage tank and the environment is:

$$\dot{Q} = \varepsilon\sigma A\left(T^4 - T_{env}^4\right) \tag{15}$$

E. THERMAL CHARACTERISTICS OF PIPELINES

The thermal characteristics of the pipeline are mainly manifested in the convective heat transfer between the cooling liquid in the tube and the tube wall, and the convective and radiative heat transfer between the tube wall and the environment. At the same time, the cooling liquid flowing in the tube will generate a certain pressure loss. The heat transfer principle of pipelines is given in Figure 3.

The Nusselt number expression for forced convective heat transfer between the tube wall and the internal coolant is:

$$Nu = 0.027\mathrm{Re}^{0.8}\mathrm{Pr}^{0.33} \tag{16}$$

The expression of the Nusselt number for the natural convection heat transfer between the tube wall and the outside

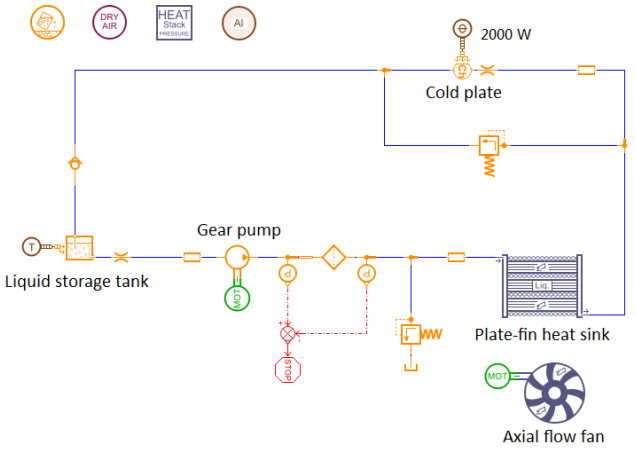

FIGURE 4. Simulation model of liquid cooling system.

air is:

$$Nu = 0.48\,(\mathrm{Pr}\,\mathrm{Gr})^{0.25} \tag{17}$$

The expression of radiant heat transfer between the tube wall and the environment is:

$$\dot{Q} = \varepsilon\sigma A\left(T^4 - T_{env}^4\right) \tag{18}$$

III. THE ESTABLISHMENT OF SIMULATION MODEL

A. SIMILATION MODEL

AMESim software is used to build simulation models of various components of the airborne liquid cooling system, which mainly include the liquid storage tank, the aircraft's reverse flight anti-overflow device, the liquid cooling pump, the pipeline oil filter, the heat exchanger, the axial fan, the cold plate, the safety valve, and other system components [26]. The system simulation model is shown in Figure 4.

The system parameters are determined based on the actual design of airborne liquid cooling system parameters. In the circuit, the axial fan is installed at the cold side air outlet of the radiator, which is used to force the radiator to cool the air. The heat exchange process mainly includes the convection exchange of the storage tank, gear pump, heat exchanger fins, cold plate, pipes, coolant, and ambient air or convection air.

B. PARAMETER SETTING

During the simulation, there is no leakage in the system, and the impurity content of the pipeline meets the actual requirements. The main working parameters of its larger thermal load components are as follows:

1) Liquid storage tank: rated working pressure 0.3 MPa, volume 4 L, cross-sectional area 175*175 mm^2, initial liquid level 100 mm, height range 80 mm-170 mm.
2) Booster pump [27]: CLB-7 type liquid cooling pump is selected, with a rated working pressure of 0.6 MPa, a rated flow of 12 L/min, and a rated power of 150 W. The main feature of the pump is that there is no shaft seal. The pump seal is realized by the combined structure of the pump and the motor. It is completely leak-free, has a wide range of use, and has high cavitation performance.
3) Coolant pipeline: inner diameter 12 mm, wall thickness 1mm.
4) Axial fan: speed 7000 r/min, power 67 W, convection air flow 710 m^3, power 67 W, impeller diameter 171.5 mm. The fan bleeds air from the environmental control system, and if necessary, can open the ram air port and let the outside air in.
5) Heat exchanger [28], [29]: SRQ-7G plate-fin heat exchanger is used, with a structure of 3 channels and 7-8-7 heat exchanger pipes, as shown in Figure 5 and Figure 6. The total heat exchange area of the coolant is 1.5 m^2, the inner pipe diameter is 9.074 mm, the pipe volume is 3.6 L, and the convection air contact area is 4.7 m^2.

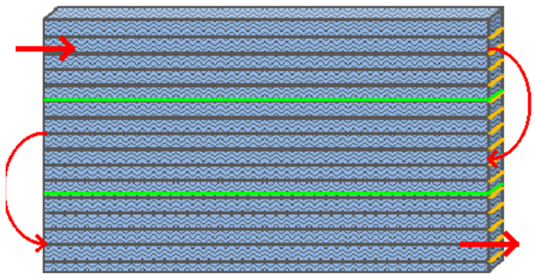

FIGURE 5. External structure of the heat exchanger.

TABLE 1. Temperature/altitude test environmental conditions.

Continuous operating temp(℃)	Requires target(℃)	The failure temperature(℃)		Flight ceiling(m)
-55.00-55.00	5.00-25.00	-60.00	85.00	15000

The main performance indicators of the system include a maximum flow rate of 12 L/min before the cold plate, and the temperature of the cold plate is maintained from 5 to 25 [30]. This article focuses on the thermal characteristics of each component to maintain the cold plate temperature within the required temperature range.

IV. SIMULATION RESULTS AND ANALYSIS UNDER TYPICAL WORKING CONDITIONS

Taking the airborne radar of a certain type of aircraft as an example, condition level 1 was selected according to the standard of airborne radar environmental conditions and test methods in [31]. The standard airborne radar temperature/altitude test environmental conditions are shown in Table 1.

In this paper, six operating temperatures of −40 °C, −20 °C, 5 °C, 10 °C, 20 °C and 40 °C, as well as flight heights of ground, 5000 m, and 10000 m, were selected as working conditions when analyzing the cooling of nose radar by the liquid cooling system. The air supply temperature of the environmental control system is 10 °C.

The temperature changes of the main components of the system at operating temperatures of 5 °C are shown in figure 7.

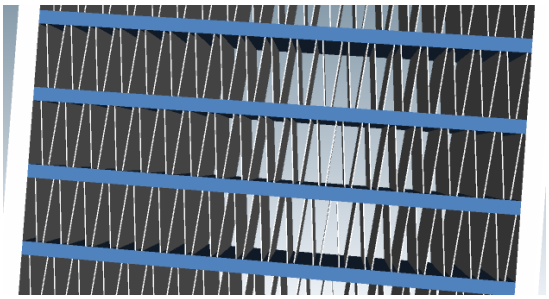

FIGURE 6. Internal structure of the heat exchanger.

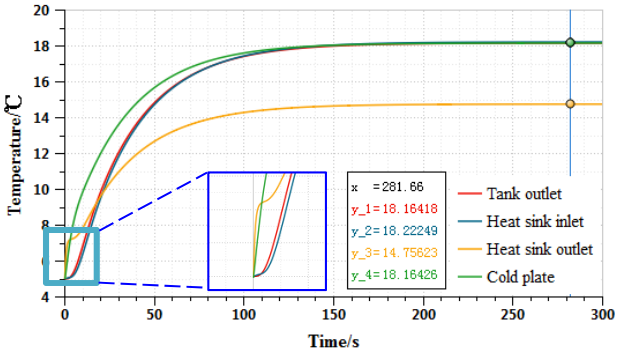

FIGURE 7. System temperature changes at 5.

TABLE 2. Stable temperature of key components.

Working temperature/ °C	Storage tank outlet temp / °C	Heat exchanger inlet temp / °C	Heat exchanger outlet temp / °C	Cold plate inlet temp / °C
-40.00	18.53	18.59	15.12	18.53
-20.00	18.35	18.42	14.95	18.36
5.00	18.17	18.23	14.76	18.17
10.00	18.13	18.19	14.72	18.13
20.00	18.12	18.18	14.56	18.12
40.00	20.55	20.58	12.68	20.61

The system starts to work and reaches a stable state after about 150 s. Considering the mechanical heat generation and pipeline loss of gear pump before the coolant enters the radiator, the inlet temperature of the radiator is the highest, higher than the outlet temperature of the liquid storage tank, and the temperature of the cold plate is close to that of the radiator outlet.

Due to the heating generated by the work of various components, when the system works at 0.87 s, the temperature at the inlet and outlet of the radiator rises briefly. Subsequently, the cooling effect of the radiator is greater than the heating effect of the coolant, and the temperature drops briefly. The cooling plate continuously transfers heat to the cooling liquid in the system, and the radiator continuously works to dissipate heat from the cooling liquid. Finally, the system temperature slowly increases to the equilibrium state. The stable temperature of the main components of the system is shown in Table 2.

Figure 8 is the thermal characteristic curve of the cold plate under the temperature condition(−40 °C-40 °C), you

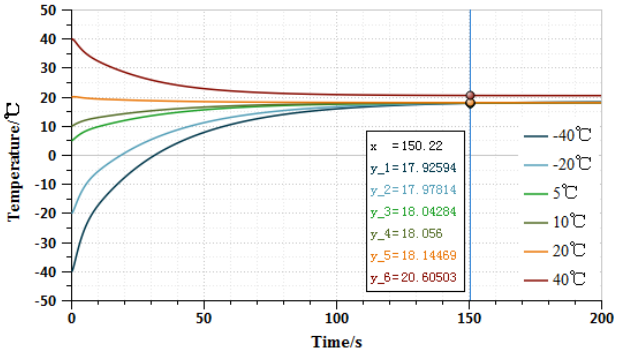

FIGURE 8. Cold plate temperature change.

can see the cold plate temperature control in 17.93 °C to 20.61 °C and stable time is about an average of 150 s, which can satisfy the cold plate inlet temperature of technical index requirements (5 °C- 25°C).

V. COMPARISON OF SEVERAL TEMPERATURE CONTROL METHODS

We compare and calculate the temperature control methods used in the system's low and high temperature conditions to determine the impact of different methods on the system's stable temperature and the rate of temperature change.

A. SYSTEM LOW TEMPERATURE

1) ELECTRIC HEATER

The method of installing a stainless steel rod-type electric heater on the lower wall plate of the liquid storage tank, and feedback control the electric heater through the temperature sensor signal of the cold plate and the outlet of the liquid storage tank. When the cold plate temperature is less than 5, the low-temperature heating relay is connected and the electric heater is turned on. When the temperature of the cold plate is higher than 16, the relay is turned off, and the electric heater stops heating. When the temperature of the storage tank is higher than 40, the overheating protection relay is turned off, and the electric heater is turned off. The temperature control is illustrated in figure 9.

The control of the electric heater is on/off position control. During the simulation process, we use the state machine in AMESim to simulate the actual electric heater temperature control. The block diagram of the state machine is presented in figure 10.

We define the temperature rise rate (K/s) as the approximate ratio of starting temperature to stable temperature and elapsed time. It can be seen from the figure 11 that the stable temperature of the cold plate at the initial temperature of −20 is about 18.3. After the temperature control of the electric heater is applied, the temperature rise rate of the cold plate is significantly faster. The rate of 18.3 °C is about 0.0089 °C/s, and the heating rate when there is an electric heater is about 0.0166 °C/s. It can also be seen from the figure 12 that the temperature rising rate without controlling the cold plate at −40 °C is about 0.1092 °C/s, and the heating

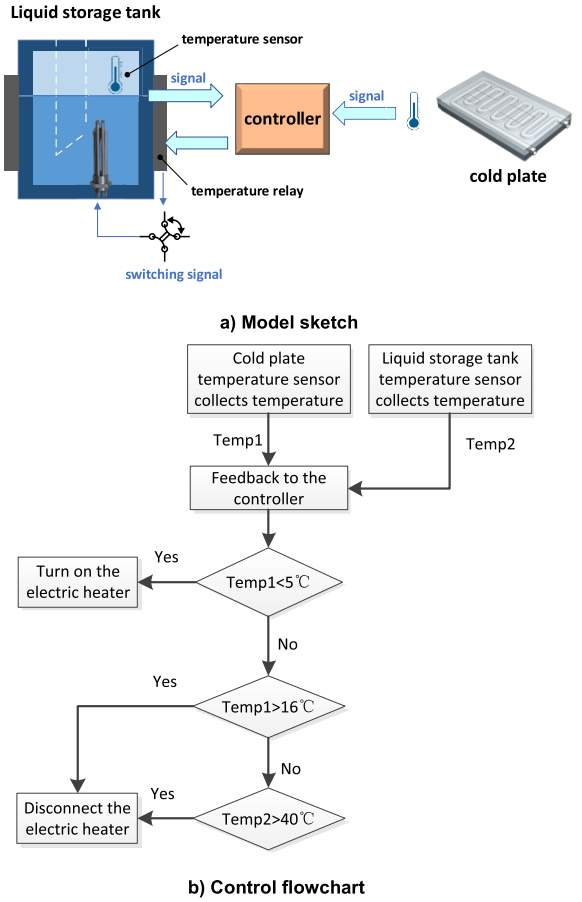

FIGURE 9. Electric heater temperature control diagram: a) Model sketch b) Control flowchart.

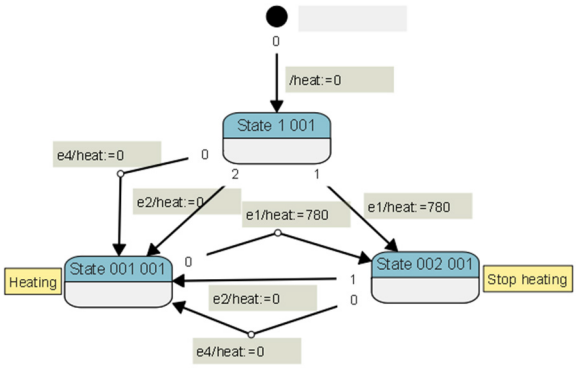

FIGURE 10. Electric heater temperature control state machine.

rate is 0.2149 °C/s when there is an electric heater. Therefore, the application of an electric heater in this type of liquid cooling source system is very useful for the rapid temperature rise of the system at a low temperature. Almost doubled.

B. SYSTEM HIGH TEMPERATURE

1) INCREASE THE FAN SPEED(METHOD 1)

It adopts segmented speed control to change the fan speed to change the fan air volume to improve the heat exchange capacity of the coolant. The maximum speed of the axial flow

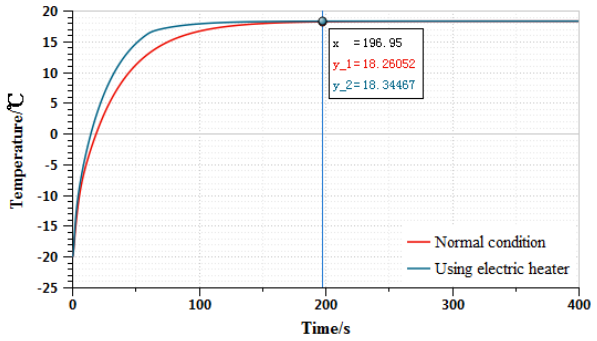

FIGURE 11. The temperature of the cold plate changes at −20.

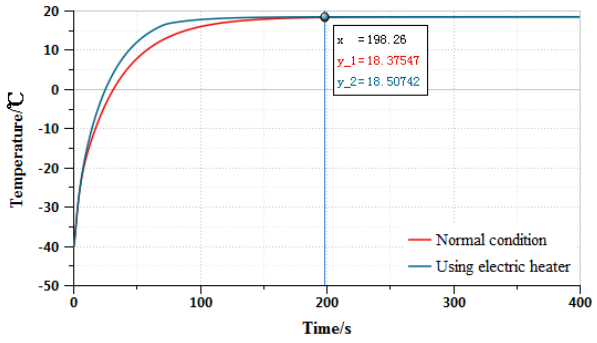

FIGURE 12. The temperature of the cold plate changes at −40.

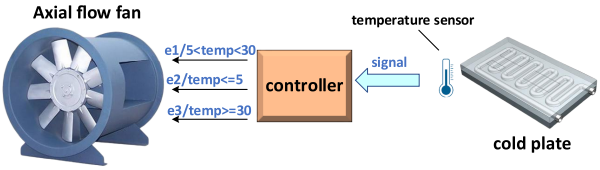

FIGURE 13. Fan speed control diagram.

fan is 7000 r/min. In AMESim, we set three gears in AMEsim, 5000 r/min, 7000r/min, and turning off the fan. The speed of the fan in three gears is adjusted to 7000 r/min when the cold plate temperature (temp) is higher than 30. When the cold plate temperature is higher than 5, the fan speed is adjusted to 5000 r/min. When the cold plate temperature is lower than 5, the fan is turned off. The speed control strategy of the fan and the block diagram of the state machine are presented in figure 13 and figure 14.

2) OPEN THE RAM AIR PORT(METHOD 2)

Under normal circumstances, during a cruise, the position of the ram air conditioning system adjustment plate is adjusted between the normal open and closed positions; during take-off and landing, the adjustment plate position is adjusted to the normal open position. When the aircraft is in the air, the baffle is retracted. Due to the low external temperature, the general adjustment plate is only fully opened for a short time when the flaps are not closed, and then closed when the flaps are closed.

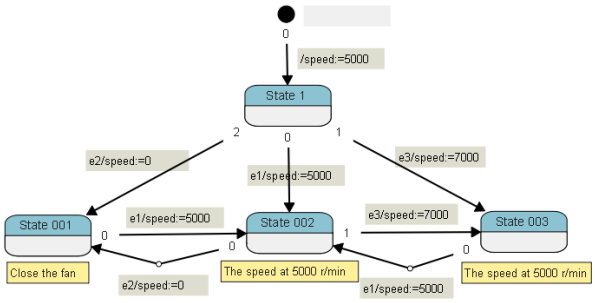

FIGURE 14. Fan speed control state machine.

TABLE 3. Cold-side gas properties in flight status [32].

Flying height	Ram air properties	Air properties after mixing
5000 m	$T_C = 255.68$ K	$T'_H = 265.33$ K
	$Q_C = 240$ kg/h	$Q'_H = 370$ kg/h
10000 m	$T_C = 223.25$ K	$T'_H = 255.03$ K
	$Q_C = 115$ kg/h	$Q'_H = 245$ kg/h

When the temperature is higher than 5, the ram air port is opened to optimize the heat dissipation effect. The state machine is packaged and added to the model as a simulation module.

Know the air inlet temperature and flow of the aircraft's environmental control system, and the temperature and flow of the ram air outlet at the corresponding altitude to obtain the mixed air temperature $T'_H(19)$, and then get the state properties of the mixed air under the flight conditions of 5000 m and 10000 m, as shown in the Table 3.

$$(T_H - T'_H) \times Q_H = (T'_H - T_C) \times Q_C \tag{19}$$

where, T_H is the air inlet temperature of the environmental control system, T_C is the air inlet temperature of the ram air port, T'_H is the air temperature after mixing.

The temperature control situation when the two systems are over-temperature is shown in figure 15 and figure 16. When the ram air port is opened under the flight altitude of 5000 m, the temperature of the cold plate drops to 7.78 °C and 10.35 °C, and method 1) drops to 19.80 °C and 20.79 °C. According to the temperature drop curve, it can be obtained that the cooling rate of normal cooling of the system at 40 °C is 0.1385 °C/s. The temperature drop rate of normal cooling of the system at 50 °C is 0.2039 °C/s, the temperature drop rate with method1 is 0.2656 °C/s, the temperature drop rate with method2 is 0.3605 °C/s. Therefore, to increase the fan speed, method1, can speed up The temperature of the cold plate decreases, but the effect is limited; method2 has a significantly better cooling effect than method1.

When the ram air port is opened at a flight height of 10000m, the cold plate temperature drops to −0.14 and 4.96. Although the temperature drops quickly, it exceeds the target requirement(5 °C-25 °C). Therefore, the method of opening

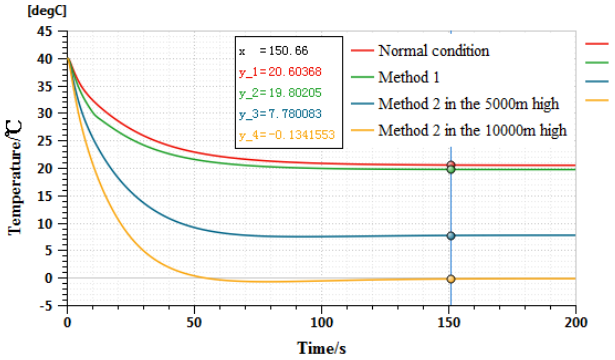

FIGURE 15. Comparison of cooling Plate cooling effects of several Schemes at 40 °C. (Normal mode refers to the situation where the system is not controlled in Section IV).

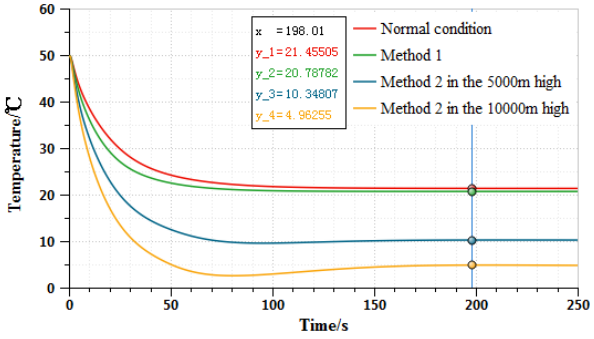

FIGURE 16. Comparison of cooling plate cooling effects of several schemes at 50 °C.

the punch air port has requirements for flight conditions, and the matching of the flight altitude and inlet flow needs to be further tested.

VI. CONCLUSION

The thermal characteristic model of the airborne liquid cooling system was established, and the dynamic changes of the temperature of the system's liquid storage tank, radiator, and mainly cold plate were calculated within the range from −40 °C to 40 °C, and several temperature control schemes were compared. We came to the following conclusions:

1) Under typical working conditions, the stable temperature of the cold plate can meet the technical requirements of cold plate inlet temperature (5 °C-25 °C).
2) Under low temperature, the control scheme of the electric heater can realize the rapid heating of the cold plate.
3) The scheme of opening the stamping air port of aircraft under high temperature has better cooling effect than the scheme of increasing the fan speed, but the former needs to consider the flight condition to avoid the cold plate temperature exceeding the index range, and the control of the inlet flow and temperature of the stamping air port needs to be further studied.

ACKNOWLEDGMENT

The authors would like to thank the anonymous reviewers for their valuable comments and suggestions.

REFERENCES

[1] J. B. Marcinichen, J. A. Olivier, and J. R. Thome, "On-chip two-phase cooling of datacenters: Cooling system and energy recovery evaluation," *Appl. Thermal Eng.*, vol. 41, pp. 36–51, Aug. 2012.
[2] J. F. Tullius, R. Vajtai, and Y. Bayazitoglu, "A review of cooling in microchannels," *Heat Transf. Eng.*, vol. 32, nos. 7–8, pp. 527–541, Jun. 2011.
[3] D.-S. Steinberg, *Vibration Analysis for Electronic Equipment*, 3rd ed. Hoboken, NJ, USA: Wiley, 1989, pp. 10–101.
[4] S.-M. Yang, W.-Q. Tao, *Heat Transfer*. Beijing, China: HEP, 2006, pp. 10–101.
[5] W. Wu, "Thermal design of airborne electronics equipment," *Piezoelectec Trics Acoustoopt.*, vol. 30, no. 2, pp. 228–229, 2008.
[6] C.-L. Zhu and X.-W. Ning, "Liquid cooling system for high-powered avionics," *J. Nanjing Univ. Aeronaut. Astronaut.*, vol. 37, no. 2, pp. 203–207, 2005.
[7] H. Y. Zhang, D. Pinjala, T. N. Wong, and Y. K. Joshi, "Development of liquid cooling techniques for flip chip ball grid array packages with high heat flux dissipations," *IEEE Trans. Compon., Packag., Technol.*, vol. 28, no. 1, pp. 127–135, Mar. 2005.
[8] H. Bostanci, D. Van Ee, B. A. Saarloos, D. P. Rini, and L. C. Chow, "Thermal management of power inverter modules at high fluxes via two-phase spray cooling," *IEEE Trans. Compon., Packag., Manuf. Technol.*, vol. 2, no. 9, pp. 1480–1485, Sep. 2012.
[9] J. Lee and I. Mudawar, "Low-temperature two-phase microchannel cooling for high-heat-flux thermal management of defense electronics," *IEEE Trans. Compon. Packag. Technol.*, vol. 32, no. 2, pp. 453–465, Jun. 2009.
[10] T. Chen and S. V. Garimella, "Flow boiling heat transfer to a dielectric coolant in a microchannel heat exchanger," *IEEE Trans. Compon. Packag. Technol.*, vol. 30, no. 1, pp. 24–31, Mar. 2007.
[11] G. Upadhya, M. Munch, P. Zhou, J. Hom, D. Werner, and M. McMaster, "Micro-scale liquid cooling system for high heat flux processor cooling applications," in *Proc. 22nd Annu. IEEE Semiconductor Thermal Meas. Manage. Symp.*, Mar. 2006, pp. 116–119 and 011.
[12] T. Y. T. Lee, J. A. Andrews, P. Chow, and D. Saums, "Compact liquid cooling system for small, moveable electronic equipment," *IEEE Trans. Compon., Hybrids, Manuf. Technol.*, vol. 15, no. 5, pp. 786–793, Oct. 1992.
[13] C. T. Nguyen, G. Roy, C. Gauthier, and N. Galanis, "Heat transfer enhancement using Al_2O_3–water nanofluid for an electronic liquid cooling system," *Appl. Thermal Eng.*, vol. 27, nos. 8–9, pp. 1501–1506, Jun. 2007.
[14] J. Y. Chang, H. S. Park, J. I. Jo, and S. Julia, "A system design of liquid cooling computer based on the micro cooling technology," in *Proc. 10th IEEE Intersoc. Conf.*, May 2006, pp. 157–160.
[15] E.-Q. Zhu, "Development of liquid cooling source control system," M. S. thesis, NJUST, Nanjing, China, 2011.
[16] Y. J. Kim, M. Jeong, Y. G. Park, and M. Y. Ha, "A numerical study of the effect of a hybrid cooling system on the cooling performance of a large power transformer," *Appl. Thermal Eng.*, vol. 136, pp. 275–286, May 2018.
[17] J. Min, "Research on control and simulation of evaporative refrigeration cycle system of fighter," Ph.D. dissertation, UESTC, Chengdu, China, 2009.
[18] G.-T. Li, "The simulation and research of small liquid cooling system," M.S. thesis, NUAA, Nanjing, Jiangsu, China, 2012.
[19] Y.-X. Li, P. Quan, L.-Z. Li, and L. Juan, "Dynamic numerical investigations of on-board vapor-compression refrigeration system," *J. Nanjing Univ. Sci. Technol.*, vol. 37, no. 1, pp. 127–132, 2013.
[20] B.-L. Zuo, X.-B. Su, K.-Q. Cao, and N. Li, "Design and simulation of liquid cooling source system based on AMESim," *Mach. Tool Hydraul.*, vol. 42, no. 16, pp. 78–81, 2017.
[21] J. B. Marcinichen, R. L. Amalfi, and N. Lamaison, "Two-phase liquid cooling system for electronics, part 4: Modeling and simulations," in *Proc. ITerm*, 2017, pp. 696–705.
[22] G. C. Birur, T. W. Sur, A. D. Paris, P. Shakkottai, and S. I. Haapanen, "Micro/nano spacecraft thermal control using a mems-based pumped liquid cooling system," *Proc. SPIE*, vol. 4560, pp. 196–206, Sep. 2001.
[23] D. Pal and M. Severson, "Liquid cooled system for aircraft power electronics cooling," in *Proc. ITherm*, Orlando, FL, USA, 2017, pp. 800–805.
[24] *2009 ASHRAE Handbook-Fundamentals*, ASHRAE, Atlanta, GA, USA, 2009.
[25] A. Y. Cengel, *Heat Transfer: A Practical Approach*. Columbus, GA, USA: McGraw-Hill, 2003.
[26] F.-Y. Ling and Q.-X. Ye, *Modeling and Simulation of AMESim System: From Introduction to Mastery*. Beijing, China: Beihang Univ. Press, 2006, pp. 20–51.
[27] Z.-H. Gao and S.-D. Jiang, "Development of 1(1/4) CLB-0.75 magnetic pump," *Fluid Machinery*, vol. 64, no. 7, pp. 17–20, 1985.
[28] S. Y. Kim, J. W. Paek, and B. H. Kang, "Flow and heat transfer correlations for porous fin in a plate-fin heat exchanger," *J. Heat Transf.*, vol. 122, no. 3, pp. 572–578, Aug. 2000.
[29] M. M. Abu-Khader, "Plate heat exchangers: Recent advances," *Renew. Sustain. Energy Rev.*, vol. 16, no. 4, pp. 1883–1891, May 2012.
[30] *Thermal Design Handbook for Reliability of Electronic Equipment*, Commission Sci. Technol. Ind. Nat. Defense., Beijing, China, 1994, pp. 40–42.
[31] *Environmental Condition and Test Methods for Aircraft Radar*, Standard SJ20115.2-92, Military Standard for Electronic Industry of the People's Republic of China.
[32] Y.-L. Li, *Research on the Key Technology of Temperature Environmental Adaptability Engineering of Aircraft Hydraulic System*. Xi'an, China: National Defense Industry Press, 2001, pp. 15–34.

ZHANGZHI DONG was born in Nanchang, China, in 1996. He received the B.S. degree in aircraft propulsion engineering, in 2018. He is currently pursuing the M.S. degree in aircraft design with Air Force Engineering University, China. He is the author of two articles. His research interests include aircraft fluid transmission and control and aviation simulation.

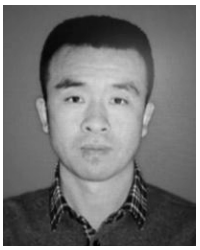

XIAOGANG LI was born in 1977. He received the Ph.D. degree in aircraft design from the College of Aeronautics, Northwestern Polytechnic University, in 2019. He is currently an Associate Professor with the College of Aeronautical Engineering, Air Force Engineering University. His main research interests include aircraft fluid transmission and control and flight dynamics modeling.

ZHE LI was born in Xinxiang, China, in 1989. He received the Ph.D. degree in aerospace science and technology from Air Force Engineering University, China, in 2019. Since June 2019, he has been a Lecturer with the Aircraft Engineering Department, Air Force Engineering University. He is the author of two books and ten articles. His research interests include flight modeling and simulation, flight risk quantification, flight safety, accidents evolution process repetition, and design of flight control law.

YANYAN HOU received the B.S. degree in electrical engineering and automation and the M.S. degree in control theory and control engineering from the Shaanxi University of Science and Technology, Xi'an, China, in 2003 and 2008, respectively.

Since 2015, she has been an Associate Professor with the College of Aeronautical Engineering, Air Force Engineering University. Her research interests include avionics mechatronics and flight dynamics modeling.